The Effective Radius in Ice Clouds

KLAUS WYSER

Department of Meteorology, Stockholm University, Stockholm, Sweden

(Manuscript received 3 March 1997, in final form 3 September 1997)

ABSTRACT

The effective radius (r_e) is a measure of the particle size used to calculate the optical properties of clouds. The objective of this study is to derive r_e from the microphysical composition of ice clouds. All ice crystals are assumed to be hexagonal columns with an aspect ratio depending on their size. Several existing particle size distributions are evaluated. The shape of the spectra is considered to be unsatisfactory for small particles and a new distribution is suggested that includes a Γ distribution for small crystals. The suggested spectrum agrees well with observations, although it is still speculative for small particles due to the limited availability of data.

The effective radius for nonspherical particles is not uniquely defined, and several possible definitions for r_e are tested. Large differences in r_e arise from the different definitions even if the same assumptions on the shape and the size distribution of ice particles are used. Norming factors help to adjust the differently defined r_e in order to make r_e from different sources compatible.

Finally, a new parameterization for r_e is suggested to avoid the expensive explicit computation. The proposed parameterization makes r_e a function of both the ice content and the temperature. A fair agreement between parameterized and observed r_e is found.

1. Introduction

Clouds interact with solar and terrestrial radiation and thereby influence the energy budget of the earth. The importance of ice clouds for the climate has been recognized for a long time (e.g., Liou 1986). Many questions concerning the microphysical composition of ice clouds have not been solved yet since it is difficult to measure ice crystals in nature. In general, ice clouds are found in the upper part of the troposphere, requiring aircrafts suited for this height. Low water vapor content and a low abundance of ice nuclei contribute to the low concentration of ice crystals that make their observation difficult. An exception might be tropical anvils or cirrus clouds originating thereof, whose composition and ice load is strongly controlled by the vertical transport from the lower troposphere. Another difficulty is the measurement of the ice particle size with scattering probes like the Forward Scattering Spectrometer Probe (FSSP) since nonspherical particles produce a complicated signal in the detector. Nonscattering optical probes like 2D arrays can sample irregularly shaped crystals, but their detection limit used to be high, typically on the order of some 10 μm. New techniques like the video ice particle sampler (VIPS, McFarquhar and Heymsfield 1996) or the counterflow virtual impactor (CVI, Noone et al. 1993) have been developed to sample micron-sized particles, but the available data are not conclusive yet. The size distribution is still very speculative and better data are highly desired, especially for small ice particles.

If large-scale models treat ice clouds at all, they often do not take into account the varying size of the ice particles in their radiation calculation. Recently, new radiation schemes have been developed that accept the size of ice crystals as an input parameter (e.g., Ebert and Curry 1992; Fu 1996). The effective radius (r_e) is a measure for the mean size in a particle population. The extinction of radiation by a particle is governed by the cross-section area of the particle (Liou 1992). In the case of spherical particles (e.g., water droplets) this leads to the well-known expression for the cross-section area weighted mean radius,

$$r_e = \frac{\int r\,\pi r^2 n(r)\,dr}{\int \pi r^2 n(r)\,dr} = \frac{\int r^3 n(r)\,dr}{\int r^2 n(r)\,dr}, \qquad (1)$$

where r is the radius and $n(r)$ is the particle distribution with respect to r. The situation becomes more complicated for nonspherical particles like ice crystals. Nonspherical particles do not have a well-defined radius; instead, their size distribution is usually defined with respect to their maximum dimension or length (L), where $n(L)dL$ is the number of particles per unit volume with length between L and $L + dL$. The integration over

Corresponding author address: Dr. Klaus Wyser, Department of Meteorology, Stockholm University, S-106 91 Stockholm, Sweden.
E-mail: klaus@misu.su.se

the size spectrum becomes $\int n(L)dL$, accordingly. The average size of an ice crystal is not uniquely given by L but should also contain information about its shape. In the simplest case this information is given by the minimum dimension or width (D) of the crystal. However, the definition for r_e is not unambiguous even if both L and D are known since (1) is valid for spherical particles only. A multitude of possible interpretations of (1) for nonspherical particles has evolved and will be discussed in section 4.

The objective of this study is to find a parameterization of r_e for ice clouds in large-scale models. The problem is split into two parts, namely, to define a size distribution of ice particles and to examine the effect of the different definitions for r_e. Existing parameterizations of the particle size distribution $n(L)$ do not take into account small ice crystals. Therefore, a new parameterization for $n(L)$ is suggested that includes also small particles. The suggested size distribution is a function of the macroscopic variables temperature (T) and ice water content (IWC). The different interpretations of the theoretical definition (1) lead to large differences in the resulting r_e. It is possible to find norming factors that allow us to compare r_e from the different definitions. Finally, a parameterization for r_e in terms of large-scale variables is sought to replace the expensive explicit calculation of r_e in ice clouds. A fair agreement is found between observed and calculated r_e.

2. Shape of ice crystals

Ice crystals occur in many different shapes or habits. Early works suggest that the ambient temperature decides the crystal type (Ono 1970), but more recent research indicates that the growth processes leading to the different habits are complicated and no simple relationship between temperature and habit exists (Dowling and Radke 1990). Despite the variety of naturally occuring habits, all crystals are treated as hexagonal columns for the remainder of this work. This simplification is chosen to make r_e from the present work applicable in the radiation scheme of Ebert and Curry (1992), which has been developed with the same assumption. The restriction to one habit is inconsistent with observations; nevertheless, radiation schemes suitable for large-scale models have yet to be developed for other habits than hexagonal columns.

The volume (V) and surface area (A) for a hexagonal, symmetrical column with length L and width D become

$$V = \frac{3\sqrt{3}}{8}D^2L, \quad \text{and} \tag{2}$$

$$A = 3\left(\frac{\sqrt{3}}{4}D^2 + DL\right). \tag{3}$$

The cross-section area (C) of a randomly oriented convex particle is equal to one-quarter of its surface area and becomes for a hexagonal column (Takano and Liou 1989)

$$C = A/4 = \frac{3}{4}\left(\frac{\sqrt{3}}{4}D^2 + DL\right). \tag{4}$$

The relationship between the length and the width of a solid column is defined as

$$\frac{L}{D} = \begin{cases} 1, & L < 30\ \mu\text{m}, \\ 1 + 0.003(L - 30\ \mu\text{m}), & L \geq 30\ \mu\text{m}. \end{cases} \tag{5}$$

Expression (5) is close to the aspect ratio suggested by Ebert and Curry (1992) except that it is continuous for all crystal sizes.

The mass of an ice crystal is the product of its density with its volume; both are parameterized as functions of L (Pruppacher and Klett 1978):

$$m(L) = \rho(L)V(L) = 2.311 \times 10^{-2}\ (L/10^4)^{2.7625}, \tag{6}$$

where m is in grams and L is in microns. The parameters in (6) have been chosen for cold, solid columns with $L/D > 2$.

3. Size spectrum

The difficulties of measuring the size distribution in ice clouds have been mentioned in the introduction. Several mathematical expressions for the size spectrum have been suggested based on observations. The limited number of data and the hardly understood variability of ice clouds make a universal size distribution difficult to find. However, large-scale models do not resolve the microphysics explicitly and the spectrum has to be parameterized, that is, an assumption on the shape of the distribution has to be made. A variety of suitable mathematical functions is presented below and compared to observations.

All parameterizations of the size spectrum are of the form $n(L) = A_x n_x(L)$, where $n_x(L)$ denotes a specific mathematical function describing the distribution. Since large-scale models usually provide information about the ice content the free parameter A_x is linked to the ice content,

$$\text{IWC} = \int m(L)A_x n_x(L)\ dL, \tag{7}$$

which is inverted to yield

$$A_x = \text{IWC}^{-1} \int m(L)n_x(L)\ dL. \tag{8}$$

Note that the major contribution to the IWC comes from large crystals, whereas the optical properties (e.g., solar albedo) are strongly controlled by the small particles (Zender and Kiehl 1994). Large errors in the computed radiative fluxes are possible since any error in IWC leads to the wrong number of ice particles, either a few large

or many small crystals, and the response in the optical properties is completely different for the two cases. The quality of the modeled radiation will certainly improve if information about ice nuclei and ice particle number concentration, possibly as a function of cloud age and history, becomes available.

a. Γ distribution

Mitchell (1994) describes the ice crystal spectrum with a Γ distribution,

$$n(L) = A_\Gamma L^{\nu_\Gamma} \exp(-\lambda_\Gamma L) \tag{9}$$

and suggests to set $\nu_\Gamma = 1$, based on observed spectra from Sassen et al. (1989). Here, two more values, 0 and -1, are assigned to ν_Γ to extend the variability of the Γ distribution. The dataset from Heymsfield and Platt (1984) includes observed values for $N_{100} = n$ (100 μm) and $\mathrm{IWC}_{\mathrm{obs}}$ as a function of temperature. To calculate IWC with (7), it is assumed that the integration over L extends from 10 to 1000 μm. A discussion of the choice of the integration limits is given in section 5. Values for λ_Γ are then found by numerically minimizing:

$$\min_{\lambda_\Gamma}\left(\frac{N_{100}}{\mathrm{IWC}_{\mathrm{obs}}} - \frac{A_\Gamma 100^{\nu_\Gamma} \exp(-100\lambda_\Gamma)}{A_\Gamma \int L^{\nu_\Gamma} \exp(-\lambda_\Gamma L) m(L)\, dL}\right)^2. \tag{10}$$

It appears that λ_Γ is not very sensitive to the temperature and, thus, can be chosen independent of T. The values found for λ_Γ are

ν_Γ	$\lambda_\Gamma[\mu\mathrm{m}^{-1}]$
1	1.27×10^{-2}
0	8.45×10^{-3}
-1	4.63×10^{-3}.

b. Exponential distribution

Ryan (1996) suggests that $n(L)$ follows an exponential distribution,

$$n(L) = A_{\mathrm{exp}} \exp(-\lambda_{\mathrm{exp}} L), \tag{11}$$

in particular for particles with L larger than about 150 μm. The form of the exponential distribution is equal to the Γ distribution with $\nu = 0$, as described above, but λ_{exp} is chosen in a different way than λ_Γ. According to Fig. 8 in Ryan (1996), λ is a function of temperature, and a visual fit to the data in the figure yields

$$\lambda_{\mathrm{exp}} = 10^{(278-T)/40} \times 10^{-3}, \tag{12}$$

where T is in kelvins and λ_{exp} in inverse microns. The available data extends only down to -25°C, and a linear extrapolation to colder temperatures is doubtful, as will be seen later.

c. Power-law distribution

The power-law spectrum is taken from Heymsfield and Platt (1984), who fitted power functions to observed size distributions,

$$n(L) = A_{\mathrm{P}} L^{B_{\mathrm{P}}}, \tag{13}$$

where both A_{P} and B_{P} are functions of T. For a good agreement between observations and (13), it is necessary to split up the spectrum in two parts: one for large and one for small particles. The parameter B_{P} is taken directly from Heymsfield and Platt, and A_{P} used here is equal to the original A multiplied by IWC.

d. Mixed distribution

Heymsfield and Platt (1984) used only particles larger than 20 μm to derive the power-law distributions. Observations show that the distribution of small particles is described fairly well with a Γ distribution (Platt et al. 1989; Moss et al. 1996; Ström et al. 1997). It is thus suggested that $n(L)$ is a combination of a Γ distribution for small particles up to 20 μm and a power-law distribution for the larger particles.

The power-law spectrum has the same functional form as (13), but the parameter B is chosen differently. Data gathered during the Central Equatorial Pacific Experiment (CEPEX) reveal that B depends on both T and IWC. The variability of B may be described by

$$B = -2 + 10^{-3}(273 - T)^{1.5} \log_{10}\left(\frac{\mathrm{IWC}}{\mathrm{IWC}_0}\right), \tag{14}$$

where T is in kelvins, IWC is in g m^{-3}, and $\mathrm{IWC}_0 =$ 50 g m^{-3}. Expression (14) has been derived from data courtesy of A. Heymsfield. The functional form of B broadens the spectrum for higher T and/or higher IWC in agreement with current understanding of cloud microphysics.

The total mixed spectrum becomes

$$n(L) = \begin{cases} A_{\mathrm{M}} L^{\nu} \exp(-\lambda L), & L \le 20\ \mu m, \\ \alpha A_{\mathrm{M}} L^{B}, & L > 20\ \mu m, \end{cases} \tag{15}$$

where α is chosen as to make $n(L)$ continuous at 20 μm. The values for ν and λ, 3 and 0.3 μm^{-1}, respectively, are kept constant. The limited amount of available data on the distribution of small ice crystals does not allow for a more sophisticated parameterization of the small particles.

e. Comparison of the distributions

All spectra described above are tested against observations. The dataset from Heymsfield and Platt (1984) is a composition of several observations, and two additional case studies are taken from Sassen et al. (1989). Figure 1 shows the distributions for two different temperature intervals with IWC taken from Heymsfield and

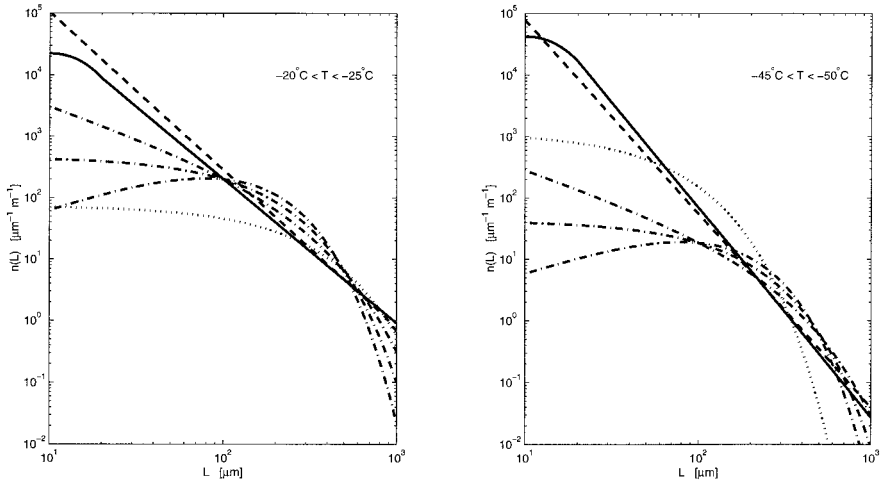

FIG. 1. Comparison of different calculated spectra with data for IWC and T taken from Heymsfield and Platt (1984). The left frame shows $n(L)$ for the temperature interval $-20°$ to $-25°$C, the right frame for $-45°$ to $-50°$C. Shown are Γ distributions (dashed–dotted), exponential (dotted), power-law (dashed), and the mixed distribution (solid) as suggested in this work. The power-law distribution is the fit of Heymsfield and Platt to the observations and, hence, is close to the true spectra.

Platt. All spectra are in close agreement for L larger than about 100 μm with the exception of the exponential distribution in the lower temperature range. The exponential distribution underestimates the number of large particles substantially for T below about -30°C. As stated above, the data for λ_{exp} is available only down to -25°C, which might explain the worse agreement of (11) for lower temperatures. Hence, the exponential distribution with λ_{exp} from (12) is not useful for the purpose of this work.

From Fig. 1 it also follows that the concentration of small particles is lower with any of the Γ distributions compared to the power-law or mixed distribution. The difference between the distributions yields different total particle concentrations, given by

$$N_{tot} = \int_{L_{min}}^{L_{max}} n(L)\, dL. \tag{16}$$

TABLE 1. Ice particle number concentration (N_{tot}) in L^{-1}, observed on 17 October 1983 (Sassen et al. 1989) and calculated with the distributions as given in the text. The upper and lower half of the table are for different assumptions on the lower integration limit L_{min}.

T (°C)	Observed	Γ, $\nu = 1$	Γ, $\nu = 0$	Γ, $\nu = -1$	Power law	Mixed
$L_{min} = 10$ μm						
−30–−35	5.8	11.0	6.8	5.9	44.5	128.8
−35–−40	4.5	4.5	2.8	2.4	37.4	108.9
−40–−45	8.9	9.8	6.0	5.2	619.1	318.2
−45–−50	5.9	6.0	3.7	3.2	304.7	372.5
−50–−55	3.3	2.3	1.4	1.2	576.9	293.8
$L_{min} = 100$ μm						
−30–−35	5.8	4.8	4.8	5.1	6.0	9.7
−35–−40	4.5	1.9	2.0	2.1	4.4	5.9
−40–−45	8.9	4.2	4.3	4.6	16.4	14.9
−45–−50	5.9	2.6	2.6	2.8	9.2	12.5
−50–−55	3.3	1.0	1.0	1.1	5.8	6.2

Table 1 shows a comparison between observed (Sassen et al. 1989) and calculated N_{tot} from the different suggested spectra. Only one case reported by Sassen et al. is displayed in the table; the results of the comparison in the other case (8 March 1985) are comparable to the ones shown here. Equation (16) is evaluated with an upper integration limit $L_{max} = 1000$ μm and a lower limit L_{min} of either 10 or 100 μm. All distributions yield comparable particle concentrations in the case $L_{min} = 100$ μm, and the results agree with the observations. Extending the integration down to 10 μm has only minor impact on the concentrations from the Γ distributions, but the changes are large for the power-law and mixed distributions. Sassen et al. (1989) state that their measurements were not accurate below 100 μm and probably underestimate the number of small particles. On the contrary, the power-law distribution is based on observations that are trustworthy down to 20 μm (Heymsfield and Platt 1984). These two reasons give strong evidence that the Γ distributions, which reproduce closely the observations of Sassen et al., give too-low values for the concentration of small particles, at least for the setting of ν used here.

The mixed distribution agrees well with the power-law distribution for large L and gives slightly lower values for $n(L)$ for small L. There are indications that the mixed distribution is more likely, especially in the small particle region. For small L the distribution must remain bounded to keep $\int n(L)\, dL$ finite. Theory also predicts that the smaller a particle, the faster it grows by vapor deposition and, hence, the number of small

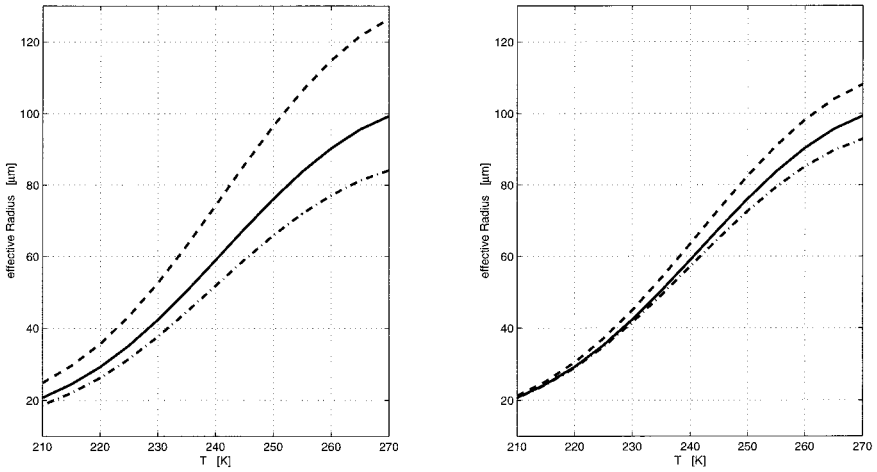

FIG. 2. Effective radius as a function of T for the different definitions of r_e from Ebert and Curry (1992, dashed), from Foot (1988, dashed–dotted), and for the definition (20) suggested here (solid). The same $n(L)$ and IWC has been used for all three curves. The left frame shows r_e for the three definitions, whereas it has been multiplied with the norming factors (29) and (30) in the right frame.

particles is depleted toward larger sizes. These requirements for the shape of $n(L)$ are fulfilled by the mixed but not by the power-law distribution.

The sum of all arguments favors the mixed distribution for the particle spectrum, and (15) is chosen to describe the distribution of ice particles for the remainder of this work. However, note that (15) represents a theoretical distribution and might differ from any actual observation, but, on the other hand, should give reasonable spectra for a variety of ambient conditions. The suggested values for the parameters $B(T, \text{IWC})$, ν, and λ were used to compute $n(L)$, which was then compared to observations and showed a fair agreement. Nevertheless, the available data on particle spectra, especially for small particles, are still limited and, consequently, the settings for the parameters remain uncertain.

4. Effective radius for nonspherical particles

The effective radius for spherical particles (1) is defined as the cross-section weighted mean radius (Liou 1992). For nonspherical particles (1) has been interpreted in various ways. Ebert and Curry (1992) calculate r_e from equivalent surface area spheres,

$$r_{e,\text{EC}} = \frac{1}{(4\pi)^{1/2}} \frac{\int A^{3/2} n(L)\, dL}{\int An(L)\, dL}. \tag{17}$$

According to Foot (1988), r_e is proportional to the ratio of the mass-equivalent sphere to the cross section of the particle:

$$r_{e,\text{FT}} = \frac{3}{4} \frac{\int Vn(L)\, dL}{\int Cn(L)\, dL}. \tag{18}$$

Both definitions (17) and (18) do not fulfill the requirement for r_e to be the cross-section weighted mean radius. Thus, a third definition is suggested here based on a proposition by Liou (1992), who assumes that the mean radius of any particle is proportional to $(DL)^{1/2}$. However, this is true only for crystals with their major axis oriented perpendicular to the incident radiation. The mean radius for a randomly oriented ice particle might be better approximated by

$$r = 0.5\, (D^2 L)^{1/3} \tag{19}$$

and, hence, r_e becomes

$$r_e = \frac{1}{2} \frac{\int D^2 Ln(L)\, dL}{\int (D^2 L)^{2/3} n(L)\, dL}. \tag{20}$$

All three definitions for r_e are independent of the crystal habit. Their evaluation, however, requires relationships between D, A, C, V, and L that depend on the crystal shape. Using the assumptions suggested in section 2 yields the result shown in the left frame of Fig. 2. The particle size distribution used was calculated with IWC and T from Heymsfield and Platt (1984). Large differences between the different definitions for r_e are apparent. Two consequences follow from the discrepancy:

1) a direct comparison of r_e from different sources is not possible and 2) r_e has to be chosen properly for a specific radiation parameterization. The problem has been addressed by Francis et al. (1994), who match the optical thickness of ice clouds in order to adjust r_e for different radiation schemes.

Norming factors for r_e might help to circumvent the problems arising from the different definitions. The idea is to have an easy means to convert the r_e from the different definitions into each other. Such a conversion is required to use any arbitrary r_e in a specific radiation parameterization. For example, $r_{e,\mathrm{FT}}$ has to be multiplied with the proper norming factor to be used in the parameterization from Ebert and Curry (1992). A possible normalization for r_e follows from the requirement that any definition of r_e should yield the same result for $D = L$. Note that the particles in this special case need not be spheres; they are still hexagonal columns but with an aspect ratio of 1. With $D = L$, the cross section, surface area, and volume defined in section 2 become, respectively,

$$C_{L=D} = \frac{3}{4}\left(\frac{\sqrt{3}}{4} + 1\right)L^2, \tag{21}$$

$$A_{L=D} = 3\left(\frac{\sqrt{3}}{4} + 1\right)L^2, \quad \text{and} \tag{22}$$

$$V_{L=D} = \frac{3\sqrt{3}}{8}L^3, \tag{23}$$

and, subsequently, the different r_e are

$$r_{e,\mathrm{EC}} = \left[3\left(\frac{\sqrt{3}}{4} + 1\right)(4\pi)^{-1}\right]^{1/2}\frac{\int L^3 n(L)\,dL}{\int L^2 n(L)\,dL}, \tag{24}$$

$$r_{e,\mathrm{FT}} = \frac{3\sqrt{3}}{2(\sqrt{3}+4)}\frac{\int L^3 n(L)\,dL}{\int L^2 n(L)\,dL}, \quad \text{and} \tag{25}$$

$$r_e = \frac{1}{2}\frac{\int L^3 n(L)\,dL}{\int L^2 n(L)\,dL}. \tag{26}$$

Define $r_{e,0}$ formally as

$$r_{e,0} = \frac{1}{2}\frac{\int L^3 n(L)\,dL}{\int L^2 n(L)\,dL} \tag{27}$$

based on the definition of r_e for spherical droplets and it follows

$$r_{e,0} = n_{\mathrm{EC}} r_{e,\mathrm{EC}} = n_{\mathrm{FT}} r_{e,\mathrm{FT}} = r_e, \tag{28}$$

where the norming factors are

$$n_{\mathrm{EC}} = \left[\frac{3}{\pi}\left(\frac{\sqrt{3}}{4} + 1\right)\right]^{-1/2} \quad \text{and} \tag{29}$$

$$n_{\mathrm{FT}} = \frac{\sqrt{3}+4}{3\sqrt{3}}. \tag{30}$$

Note that no norming factor is necessary for r_e defined with (20). The right frame of Fig. 2 shows r_e as a function of T for the different definitions, but now multiplied with the norming factors. The difference between the three curves is greatly reduced compared to the left frame of Fig. 2 but does not vanish entirely since the equality stated in (28) is valid only for the case $D = L$. Nevertheless, the norming factors help to make r_e from different definitions comparable and allow an easy adjustment of r_e whenever it is needed.

5. Integration limits

Any definition for r_e requires integrations over the size spectrum. Theoretically, the integration over L extends from 0 to ∞, but practically the limits are set to a finite upper and a nonzero lower value. The integration limits for all calculations in this work are set as 10 and 1000 μm, respectively, if not stated otherwise. The suggested values are assumed to be typical for ice clouds. The sensitivity of (20) to changes in the upper limit is low: r_e decreases by 20% if $L_{\max}$ is set to 600 μm and increases by 20% if it is set to 1900 μm. The sensitivity to changes of $L_{\min}$ is more crucial: r_e increases by 20% already if the lower limit is 50 instead of 10 μm. The reliability of many instruments may be doubted below typically 100 μm (e.g., Sassen et al. 1989) and many studies exclude small particles due to problems with their reliable observation. However, the small particles may make an important contribution to r_e as shown above, and their exclusion may lead to a serious bias in r_e.

Real spectra certainly have an upper limit, defined by the largest possible ice crystal. The low abundance of large particles makes their observation difficult and, consequently, the shape of the spectrum is not well defined for large particles. The upper integration limit should thus not be the size of the largest measured particle but a typical maximum size for the entire cloud.

It is difficult to measure small ice particles, and the shape of the spectrum at the lower detection limit is uncertain. New results indicate that the smallest particles in ice clouds are not a few tens of microns but rather a few microns, but the results are not conclusive yet. The setting of the lower limit is considered to be preliminary and better information about small ice crystals,

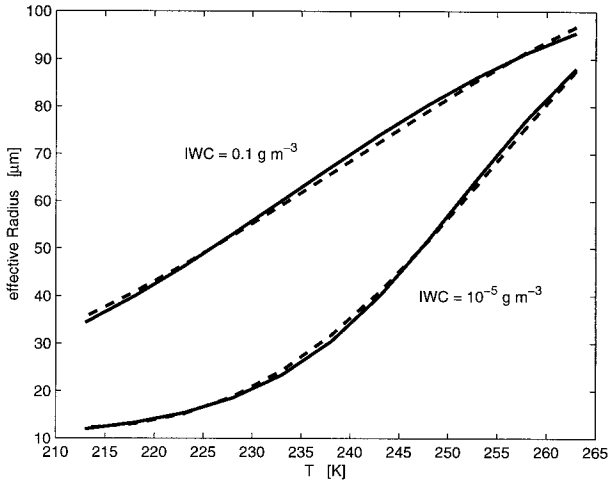

FIG. 3. Exact (solid) and parameterized (dashed) r_e according to (35) for two values of IWC.

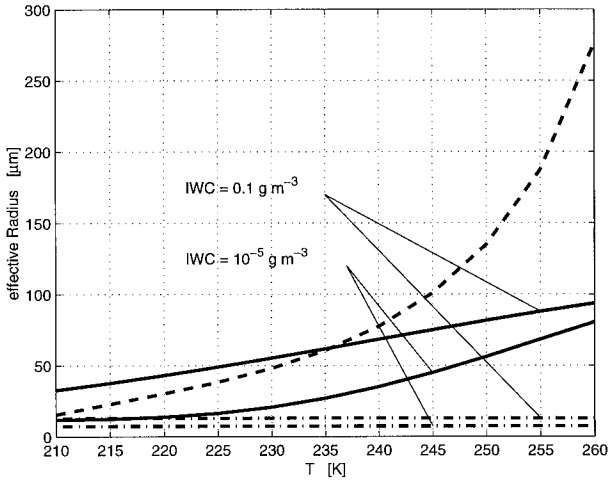

FIG. 4. Effective radius as a function of T for various parameterizations. The dashed line denotes $r_{e,\mathrm{Ou}}$, the dashed–dotted $r_{e,\mathrm{Fa}}$, and the solid the parameterization (35) suggested in this study. Two different values, 0.1 and 10^{-5} g m^{-3}, have been used for IWC. Note that $r_{e,\mathrm{Ou}}$ is independent of IWC.

from measurements or theory, is highly desired to set it properly.

6. Parameterizations for r_e

The explicit calculation of r_e is expensive and large-scale models use parameterizations instead. Several parameterizations for r_e have been developed whereof two are presented here. McFarlane et al. (1992) suggest that r_e should be a function of IWC:

$$r_{e,\mathrm{Fa}} = 5640X^{0.786}, \tag{31}$$

where the mean crystal length (X) is given by

$$X = [0.698 + 0.366 \log_{10}\mathrm{IWC} + 0.122(\log_{10}\mathrm{IWC})^2 + 0.0136(\log_{10}\mathrm{IWC})^3] \times 10^{-3} \tag{32}$$

with IWC in g m^{-3} to yield r_e in microns.

According to Ou and Liou (1995), the mean effective size (D_e in microns) depends on the temperature (T_c in °C):

$$D_e = 326.3 + 12.42T_c + 0.197T_c^2 + 0.0012T_c^3. \tag{33}$$

Ou et al. (1995) suggest a relation between r_e and D_e, which is inverted here to yield

$$r_{e,\mathrm{Ou}} = -2.2054 + 0.56383D_e + 5.6416 \times 10^{-3}D_e^2 - 3.0954 \times 10^{-5}D_e^3 + 1.2601 \times 10^{-7}D_e^4, \tag{34}$$

where r_e is in microns.

The fundamental difference between the two parameterizations is that r_e is related only to IWC in (31) and only to T in (34). In the present work $n(L)$ is assumed to depend on both IWC and T and, consequently, the parameterization of r_e should take this double dependency into account. The only step in the derivation of $n(L)$ where T and IWC appear together is (14), and, thus, the parameterization of r_e might be in terms of B. Note however that r_e also depends on the distribution of small particles, which is assumed to be independent of IWC and T. Any change in the small particle spectrum induces a change in r_e and its parameterization must be adjusted even though B remains unchanged. The parameterization for r_e is found by first calculating $n(L)$ according to (15) as a function of B in the range between -6 and -2; this $n(L)$ is then used to calculate r_e with (20). Finally, a relation between the initial B and the obtained r_e is sought and approximated with a third-order polynomial,

$$r_e = 377.4 + 203.3B + 37.91B^2 + 2.3696B^3. \tag{35}$$

Expression (35) together with (14) for $B(T, \mathrm{IWC})$ allows us to calculate r_e from T and IWC. A comparison between the exactly calculated and the parameterized r_e is shown in Fig. 3.

The different parameterizations (31), (34), and (35) are shown in Fig. 4, and the spread between them is remarkable. The parameterization suggested here yields values for r_e that lie between $r_{e,\mathrm{Ou}}$ and $r_{e,\mathrm{Fa}}$. The parameterization from Ou and Liou has been developed for temperatures below -20°C, and the large $r_{e,\mathrm{Ou}}$ at warmer temperatures might be unrealistic. Furthermore, Ou and Liou calculate r_e with a spectrum where all particles smaller than 20 μm have been neglected, which gives a positive bias for r_e (see section 5). Including smaller particles in the derivation of $r_{e,\mathrm{Ou}}$ might yield values not too different from those calculated with (35), at least for T below 253 K. Unfortunately, no details of the derivation of $r_{e,\mathrm{Fa}}$ are known, and nothing can be said about restrictions to its use or problems with possible biases.

The differences between the parameterizations pre-

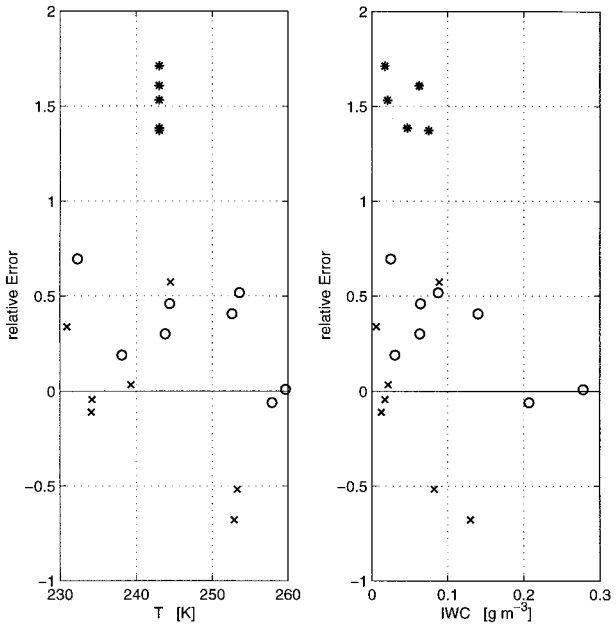

FIG. 5. The relative error Δr_e between (35) and observations made in three different ice clouds. The result is coded with respect to the observation: Stars for Gayet et al. (1996), crosses for ICE 215, and circles for ICE 217 (Francis et al. 1994).

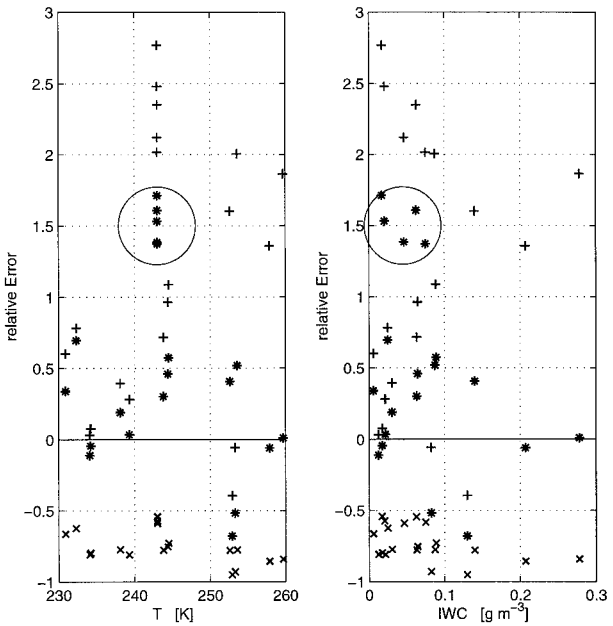

FIG. 6. As in Fig. 5, but all Δr_e obtained with (35) are shown as stars. Additionally, results obtained with the other parameterizations $r_{e,\mathrm{Fa}}$ ($\times$) and $r_{e,\mathrm{Ou}}$ ($+$) are shown. No distinction has been made for the three different observations. The points encircled are from the comparison between the paramaterization (35) and the observations of Gayet et al. (1996).

sented in this section are larger than the differences arising from different definitions for r_e in section 4 (cf. Figs. 2 and 4). It is highly probable that the different parameterizations have been developed with different assumptions on the size distributions. This last finding clearly shows the need for a reliable size spectrum in the calculation of r_e.

7. Validation

The parameterization (35) is tested against observed r_e from two recent studies, both performed in 1989 as a part of the International Cirrus Experiment (ICE). Francis et al. (1994) observed ice clouds over central Scotland (ICE 215) and over the southwestern peninsula of England (ICE 217), and Gayet et al. (1996) report on cirrus over the North Sea. The values for T and IWC in (35) are taken from the observations. As mentioned before, r_e cannot be measured directly but has to be derived from observed quantities. Assumptions on the shape or the distribution of ice crystals have a large influence on the value obtained for r_e.

Francis et al. used a 2D-C probe to measure the spectrum of particles with sizes between 25 and 800 μm. They correct the spectrum with Γ distributions for smaller and larger particles to achieve the correct IWC that was measured with another method. The corrections applied reduce r_e and the adjusted value for r_e is taken for the comparison here.

The relative difference between parameterized and observed r_e, defined as

$$\Delta r_e = \frac{r_e(\mathrm{IWC}, T) - r_{e,\mathrm{obs}}}{r_{e,\mathrm{obs}}}, \tag{36}$$

is shown in Fig. 5 as a function of T or IWC. In general, Δr_e is positive, which means that the parameterized r_e exceeds the observed. However, no general conclusion can be drawn since the variability of Δr_e is high. No correlation is found for Δr_e and T. There might be an increase in Δr_e with low IWC, but, at the same time, the variability of Δr_e increases, which makes the possible trend uncertain.

The largest Δr_e's are found with the observations of Gayet et al. (1996). The large difference might arise from the FSSP-100 that was used to detect small particles. The instrument is able to measure spherical particles down to 3 μm, but its performance with nonspherical particles is quite uncertain. It is possible that the FSSP overestimates the number of small particles, or, equivalently, the size of the measured particles, thus inducing a too-low value for r_e. Another possible explanation for the large Δr_e could be an underestimation of the concentration of large particles in the observations. Gayet et al. used a 2D-C probe with a detection range between 25 and 800 μm, and no correction was applied to include possible larger particles. Expression (35) has been developed for a maximum particle size of 1000 μm and, consequently, a slightly larger value for r_e may result from (35).

Figure 6 displays the comparison between Δr_e for the suggested parameterization (35) and for the other par-

ameterizations $r_{e,\mathrm{Fa}}$ and $r_{e,\mathrm{Ou}}$ with the same set of observations as before. The relative difference obtained with (35) is lower than that from the other parameterizations, especially if the observations from Gayet et al. (encircled in Fig. 6) are excluded from the comparison.

8. Concluding remarks

The purpose of this study is to calculate r_e in ice clouds based on information about the cloud's microphysics. The crystal habit is chosen to consist of hexagonal columns, mainly to make r_e from this study compatible with the radiation scheme from Ebert and Curry (1992). A new size distribution $n(L)$ is suggested, composed of a Γ distribution for small crystals and a power-law distribution for large crystals. The new $n(L)$ is able to reproduce observed ice spectra.

With $n(L)$ it is possible to calculate the effective radius. However, r_e depends on the definition used—that is, how the r^3 and r^2 terms in (1) are interpreted. Norming factors have been developed that allow a comparison of r_e from the different definitions. The norming factors are also useful for practical applications, for example, to apply any r_e in a given radiation scheme even if a different definition for r_e has been used to develop the scheme.

The assumptions on the shape, size distribution, and definition allow us to compute r_e explicitly, but for practical reasons a parameterization for r_e is sought. Unlike existing parameterizations, the suggested parameterization depends on both the amount of cloud ice and the temperature. A comparison with observations shows a fair agreement, although differences may be appreciable sometimes. It is not clear, however, if the parameterization or the observation fails since the interpretation of the observed shape and spectrum of ice crystals lead to a large uncertainty in the observed r_e.

The results from this study shed light on the sensitivity of r_e to the microphysical composition of ice clouds. There is a need for better data about the size distribution and shape of ice crystals in order to improve the retrieval for r_e with all its consequences for the radiation calculation. Special emphasis should be put on small particles whose reliable detection has been impossible hitherto. The small particles may make an important contribution for the radiative transfer in clouds and should not be neglected (Zender and Kiehl 1994; Arnott et al. 1994). It might be possible to gather more data from in situ observations, but the detection of small nonspherical particles is not easy.

Remote sensing techniques have a great potential to improve the knowledge about the composition of clouds (e.g., Ou et al. 1995). The transmission through and reflection in clouds can be measured directly with ground- or space-based platforms; the problem then is to solve the inverse problem, that is, to find the phase, size, and shape of the cloud particles from the observed radiation. Another promising technique is the advent of active optical sensors such as lidars—their advantage is the well-defined direction, frequency, polarization, and pulse length of the light beam, which opens new possibilities in remote sensing.

Better understanding may also come from microphysical models where crystal nucleation and growth are studied for a variety of environmental conditions. The information from these models might be used to improve the assumptions made in this study on the size distribution and, possibly, on the crystal habit.

Acknowledgments. I would like to thank Prof. H. Sundqvist and two anonymous reviewers for their critical comments that helped improve this manuscript. This study has been supported by the Swedish Natural Science Research Council (NFR) under Grant G-AA/GU02923-317.

REFERENCES

Arnott, W. P., Y. Dong, J. Hallet, and M. R. Poellot, 1994: Role of small ice crystals in radiative properties of cirrus: A case study, FIRE II, November 22, 1991. *J. Geophys. Res.,* **99,** 1371–1382.

Dowling, D. R., and F. L. Radke, 1990: A summary of the physical properties of cirrus clouds. *J. Appl. Meteor.,* **29,** 970–978.

Ebert, E. E., and J. A. Curry, 1992: A parameterization of ice cloud optical properties for climate models. *J. Geophys. Res.,* **97,** 3831–3836.

Foot, J. S., 1988: Some observations of the optical properties of clouds. Part II: Cirrus. *Quart. J. Roy. Meteor. Soc.,* **114,** 145–164.

Francis, P. N., A. Jones, R. W. Saunders, K. P. Shine, A. Slingo, and Z. Sun, 1994: An observational and theoretical study of the radiative properties of cirrus: Some results from ICE'89. *Quart. J. Roy. Meteor. Soc.,* **120,** 809–848.

Fu, Q., 1996: An accurate parameterization of the solar radiative properties of cirrus clouds for climate models. *J. Climate,* **9,** 2058–2082.

Gayet, J.-F., G. Fevbre, G. Brogniez, H. Chepfer, W. Renger, and P. Wendling, 1996: Microphysical and optical properties of cirrus and contrails: Cloud field study on 13 October 1989. *J. Atmos. Sci.,* **53,** 126–138.

Heymsfield, A. J., and C. M. R. Platt, 1984: A parameterization of the particle size spectrum of ice clouds in terms of the ambient temperature and ice water content. *J. Atmos. Sci.,* **41,** 846–855.

Liou, K. N., 1986: Influence of cirrus clouds on weather and climate processes: A global perspective. *Mon. Wea. Rev.,* **114,** 1167–1199.

——, 1992: *Radiation and Cloud Processes in the Atmosphere.* Oxford University Press, 487 pp.

McFarlane, N. A., G. J. Boer, J.-P. Blanchet, and M. Lazare, 1992: The Canadien Climate Center second-generation general circulation model and its equilibrium climate. *J. Climate,* **5,** 1013–1044.

McFarquhar, G. M., and A. J. Heymsfield, 1996: Microphysical characteristics of three anvils sampled during the Central Equatorial Pacific Experiment. *J. Atmos. Sci.,* **53,** 2401–2423.

Mitchell, D. L., 1994: A model predicting the evolution of ice particle size spectra and radiative properties of cirrus clouds. Part I: Microphysics. *J. Atmos. Sci.,* **51,** 797–816.

Moss, S. J., P. N. Francis, and D. G. Johnson, 1996: Calculation and parameterization of the effective radius of ice particles using aircraft data. *Proc. 12th Int. Conf. on Clouds and Precipitation,* Zurich, Switzerland, Int. Commission on Clouds and Precipitation and Int. Assoc. of Meteorology and Atmospheric Science, 1255–1258.

Noone, K. B., K. J. Noone, J. Heintzenberg, J. Ström, and J. A. Ogren, 1993: In situ observations of cirrus cloud microphysical properties using the counterflow virtual impactor. *J. Atmos. Oceanic Technol.,* **10,** 294–303.

Ono, A., 1970: Growth mode of ice crystals in natural clouds. *J. Atmos. Sci.,* **27,** 649–658.

Ou, S.-C., and K. N. Liou, 1995: Ice microphysics and climatic temperature feedback. *Atmos. Res.,* **35,** 127–138.

——, and Coauthors, 1995: Remote sounding of cirrus cloud optical depths and ice crystal sizes from AVHRR data: Verification using FIRE II IFO measurements. *J. Atmos. Sci.,* **52,** 4143–4158.

Platt, C. M. R., J. D. Spinhirne, and W. D. Hart, 1989: Optical and microphysical properties of a cold cirrus cloud: Evidence for regions of small ice particles. *J. Geophys. Res.,* **94,** 11 151–11 164.

Pruppacher, H. R., and J. D. Klett, 1978: *Microphysics of Clouds and Precipitation.* D. Reidel, 714 pp.

Ryan, B. F., 1996: On the global variation of precipitating layer clouds. *Bull. Amer. Meteor. Soc.,* **77,** 53–70.

Sassen, K., D. O. Starr, and T. Uttal, 1989: Mesoscale and microscale structure of cirrus clouds: Three case studies. *J. Atmos. Sci.,* **46,** 371–396.

Ström, J., B. Strauss, F. Schröder, T. Anderson, J. Heintzenberg, and P. Wendling, 1997: In situ observations of the microphysical properties of young cirrus clouds. *J. Atmos. Sci.,* **54,** 2542–2553.

Takano, Y., and K. N. Liou, 1989: Solar radiative transfer in cirrus clouds. Part I: Single-scattering and optical properties of hexagonal ice crystals. *J. Atmos. Sci.,* **45,** 3–19.

Zender, C. S., and J. T. Kiehl, 1994: Radiative sensitivities of tropical anvils to small ice crystals. *J. Geophys. Res.,* **99,** 25 869–25 880.